Whispers in the Snow: Exploring LoRa Technology for Avalanche Search and Rescue Scenarios

Michele Girolami
ISTI-CNR
Italian Research Council
Pisa, Italy
michele.girolami@isti.cnr.it

Giulio Maria Bianco
DICII
University of Rome Tor Vergata
Rome, Italy
giulio.maria.bianco@uniroma2.it

Fabio Mavilia
ISTI-CNR
Italian Research Council
Pisa, Italy
fabio.mavilia@isti.cnr.it

Gaetano Marrocco
DICII
University of Rome Tor Vergata
Rome, Italy
gaetano.marrocco@uniroma2.it

***Abstract*—This contribution outlines an experimental setup and methodology employed to extensively characterize LoRa propagation in the demanding scenario of avalanche search and rescue (SaR), where the transmitter is buried under snow. The considered scenario presents challenges, including the absence of line-of-sight between the transmitter and receiver, as well as signal attenuation due to environmental factors such as temperature, humidity, and snow conditions. We analyze the variations in Received Signal Strength (RSS) and Signal-to-Noise Ratio (SNR) with increasing distance between the transmitter and receiver. Our data collection campaign completely characterizes, for the first time, the snow type during wireless communication tests. Finally, we test the maximum distance at which the LoRa signal can be received from the buried transmitter, demonstrating the technology's potential in challenging environments.**

***Index Terms*—LoRa, ARVA, localization, search and rescue.**

I. Introduction

In recent years, Long-Range (LoRa) protocol has become one of the more commonly adopted low-power wide-area network (LPWAN) technologies because of its kilometric coverage, which is obtained from transmission powers of milliwatts. Developed in 2009 and commercialized since 2015 [1], LoRa is currently used for several applications requiring long-term monitoring, especially for distributed sensing [2], which benefits from its high-performing modulation derivative from Chirp Spread Spectrum (CSS) [3]. Sustained by the commercial success of this radiofrequency technology, new research avenues, such as specific performance evaluations [4] and channel characterization techniques using multiple chirps signals [5], are being investigated worldwide.

Among the potentially disruptive applications, LoRa can be employed for Search and Rescue (SaR) operations in avalanche scenarios where the victim and hence the transmitter are buried under snow. Indeed, state-of-the-art models in similar antenna arrangements are still preliminary and based on a relatively small number of packets or laboratory settings [6], [7], highlighting the necessity of a more thorough experimental campaign to derive a more representative propagation model. In such challenging conditions, LoRa can be adopted for fast localization and aid of persons in distress, especially when it is combined with wearable beacons and UAVs (unmanned aerial vehicles) [8], [9]. However, the performance of signal-based localization techniques, necessary for the development of LoRa-based low-cost devices, is severely hindered by the limited knowledge of radio wave propagation in harsh environments, where SaR operations occur, such as in emergency mountainous scenarios [6]. Two main technologies are currently adopted in SaR operation for avalanche events: Avalanche Transceivers also referred to as ARVA and RECCO tags. ARVA technology represents the gold-standard for avalanche rescue; however, the maximum distance between a buried transmitter and a receiver is approximately 50 m - 70 m.

Among the potentially disruptive applications, LoRa can be employed for Search and Rescue (SaR) operations in avalanche scenarios where the victim and hence the transmitter are buried under snow. Indeed, state-of-the-art models in similar antenna arrangements are still preliminary and based on a relatively small number of packets or laboratory settings [6], [7], highlighting the necessity of a more thorough experimental campaign to derive a more representative propagation model. In such challenging conditions, LoRa can be adopted for fast localization and aid of persons in distress, especially when it is combined with wearable beacons and UAVs (unmanned aerial vehicles) [8], [9]. However, the performance of signal-based localization techniques, necessary for the development of LoRa-based low-cost devices, is severely hindered by the limited knowledge of radio wave propagation in harsh environments, where SaR operations occur, such as in emergency mountainous scenarios [6]. Two main technologies are currently adopted in SaR operation for avalanche events: Avalanche Transceivers also referred to as ARVA and RECCO tags. ARVA technology represents the gold-standard for avalanche rescue; however, the maximum distance between a buried transmitter and a receiver is approximately 50 m - 70 m.

This study presents an experimental setup and the adopted methodology that we are currently employing to completely characterize, for the first time, LoRa propagation in the challenging SaR scenario of an avalanche victim with a trans-

mitter buried under snow which is contextually analyzed. This scenario is characterized by two main aspects: the absence of line-of-sight between the transmitter and receiver and signal attenuation caused by environmental conditions such as temperature, humidity and most importantly snow conditions. For this purpose, in this work, we describe our data collection campaign, which involves one transmitter and four receivers. We conduct two kinds of tests. First, we aim to characterize the LoRa propagation when the receivers are positioned at specific reference locations up to 50 m distant from the transmitter position. In particular, for each reference location, we collect data from the four receivers, and we analyze how RSS (Received Signal Strength) and SNR (Signal to Noise Ratio) vary as the distance between the transmitter and receiver increases. Second, we test the maximum distance at which we are able to receive the LoRa signal from the transmitter buried under the snow. The goal of this last test is to show the potential of the LoRa technology in the challenging scenario.

From our experiments, we observe that the LoRa signal tends to remain stable and *clear* at distances ranging from 0 m to 50 m, while concerning the maximum distance test, we are able to receive LoRa signals up to 410 m under non-line of sight conditions.

II. Related Works on LoRa for Search and Rescue

Focusing on the SaR application, recent works have mainly addressed three lines of investigation: *i*) exploiting LoRa to provide wireless connectivity, eventually by deploying a gateway, *ii*) using the LoRa signal for GPS-free localization, since in the harshest SaR scenarios satellite positioning of the victim is negated, and *iii*) improvements of LoRa devices specifically designed to support SaR missions.

Table I summarizes relevant the results in terms of the antichronological order concerning the three aspects previously mentioned. The exploitation of LoRa technology to provide extended connectivity is the most investigated research line since it is the most immediate use of those devices for such scenarios. In particular, authors in [10] collected an experimental dataset based on LoRa for SAR operations by varying the snowpack type and the burial depths. Authors detail the adopted hardware and the methodology of the data collection campaign. References [11] and [12] proposed the use of UAVs carrying LoRa gateways, and eventually Wi-Fi access points, in typical areas of intervention such as mountain canyons or forests. The use of UAVs in these cases can overcome the critical issue of difficult terrain, which could hinder ground drones while simultaneously achieving ray-paths that are less obstructed by shadowing obstacles and, hence, provide large and reliable radio coverage. Moreover, references [13] and [14] investigate the benefits of combining LoRa communication with typical GPS trackers for SaR for transmitting the location of rescue teams or the target to be rescued, whereas LoRa signals were exploited for piloting ground robots in the eventuality of hazardous indoor terrain (e.g., crumbling structures after an earthquake). A more sophisticated approach characterizes the LoRa radiowave propagation for the implementation of radiolocation techniques [6], even by exploiting flying drones [8]. Although this second approach provides many benefits because of the localization based on simple signal strength, it requires specific radiowave fading modelling, possibly also accounting for the wearer's body, since any uncertainty in the propagation model results in greater localization errors [15]. This issue is complicated by the very same use of UAVs due to the peculiarities of propagation between terrestrial radio and flying UAVs [8]. Finally, some works develop modified LoRa devices that are advantageous for SaR missions; for instance, [16] develops an energy consumption optimization algorithm to further reduce power consumption and enhance battery life.

TABLE I: Recent literature on LoRa SaR systems.

Ref.	Year	Description
[10]	2024	Experimental dataset for search and rescue operations
[8]	2023	Characterization of LoRa body-UAV EM links for SaR in Mediterranean forests.
[13]	2023	LoRa trackers for SaR-trained dogs.
[11]	2023	Flying gateway through UAV to support LoRa connectivity in SaR areas.
[17]	2022	Use of LoRa links to pilot SaR ground robots.
[14]	2022	GPS coordinates in disaster areas sent by LoRa.
[12]	2022	UAV providing LoRa and Wi-Fi connectivity to unconnected areas.
[16]	2021	LoRa devices with increased battery life developed for SaR missions.
[6]	2021	LoRa system with localization algorithm for mountain SaR.

The present work is instrumental for the first two research lines, since the characterization of electromagnetic (EM) links is vital for correctly deriving the LoRa radio range expected in the actual emergencies and to apply several GPS-free localization techniques, such as classical techniques based on the RSS [18]. Our work differs from those of existing papers in two main ways. On the one hand, we set-up a reproducible data collection campaign characterized by several testing locations and an accurate snow profile report provided by ARPAV[1]. We also detail the adopted methodology and the setup. On the other hand, we show the potential of LoRa technology by measuring the maximum distance between a buried transmitter and a receiver in an avalanche scenario.

III. Experimental Settings

In this section, we describe our data collection campaign reporting the adopted hardware and software as well as the methodology and the experimental area.

[1]Unità Organizzativa Neve, Valanghe e Stabilità dei Versanti - Centro Valanghe di Arabba.

(a)

(b)

Fig. 1: The adopted transmitter and receiver.

TABLE II: CONSIDERED LORA TRANSMISSION PARAMETERS.

Transmission Parameter	**Value**	**Transmission Parameter**	**Value**
Transmission power	14 dBm	Bandwidth	125 kHz
Carrier frequency	868 MHz (EU)	Coding rate	4/5
Spreading factor	7	Message rate	3 Hz

A. Hardware and Software

The hardware utilized in the experimental setup consists of 5 T-beam meshtastic boards (by LILYGO) [19] that include the chipsets ESP32 and SX1276. The T-beam boards are equipped with GSM/GPRS Antenna L722 (by LILYGO) [20] and are powered by power banks with a battery capacity of 30000 mA/h. One board transmits while the other board receives through *raw LoRa* [6], viz., broadcasting the packets bypassing the MAC layer. The transmitter is positioned in a water-proof bag and buried under snow, as shown in Fig. 1a. Receiver boards were connected to Raspberry Pi 4 to store the characteristics of the packets (timestamp, RSS, and SNR) on SD memory cards in text files. Receivers are synchronized through an initial connection to a laptop computer via the Wi-Fi and NTP protocols. All the antennas are placed to be vertically-polarized to characterize the propagation of the EM wave. Fig. 1b shows the receiver mounted on top of a tripod used for data collection. Both the transmitter and the receivers are programmed with custom firmware whose goal is to emit simple LoRa messages at periodic intervals and to receive LoRa messages and log RSS and SNR values. We configure the firmware with the transmission parameters reported in Table II. In particular, we decide to set SF=7 (spreading factor), the transmission power set to 14 dBm, and the coding rate set to 4/5.

We also adopt a simple Android-based application to keep track of the starting and ending time for each data collection in the different reference locations (see Section III-B). The mobile application runs on a Google Pixel 6-pro whose clock is synchronized with the NTP protocol.

Fig. 2: The experimental area equipped with reference locations.

TABLE III: Adopted terminology for snow profile characterization (from the ICSI-UCCS-IACS 2009 standard).

Symbol	**Description**	**Units or classes**
H	Snow height	cm from ground
T_a, T_N	Temperature (air and snow)	°C
F	Snow grain shape	9 classes from the standard
E	Snow grain dimension	mm; length of the major axis
R	Snow hardness	From 1 (very soft) to 6 (ice)

B. Methodology and Experimental Area

The data collection campaign is designed considering four main requirements:

1) identifying an experimental area enabling us to deploy a number of reference locations on the ground;
2) testing the LoRa propagation under different environmental conditions;
3) reaching the maximum admissible distance between the LoRa transmitter and receiver;
4) recording the snow profile during the data collection for snow characterization.

For this purpose, we identify a plateau located at Col de Mez (Falcade, Italy)[2] at 1870 m above sea level, as shown in Fig. 2.

C. Characterization of the Snow Profile

During our tests, we recorded the snow profile according to AINEVA's model 4[3]. The snow profile allows describing, according to a shared taxonomy and classification, the snow properties following the International Classification for Seasonal Snow on the Ground ICSI-UCCS-IACS 2009[4]. By characterizing snow, we can enhance our understanding of how it impacts the propagation of collected LoRa signals, thereby improving our grasp of their properties. We report below a description of the snow profile, by using the terminology reported in the ICSI-UCCS-IACS, as summarized in Table III.

Tests and snow profile data are collected on January 24, 2024, at 11:30 AM. The recorded temperature was +9°C, and the snow profile is executed in a flat area (0° inclination) of Plan de Mez (see Section III-B), which is exposed to the

[2]GPS coordinates: 46°22'41", 11°49'33"
[3]https://aineva.it/wp-content/uploads/2020/02/Modello4vrs2013.pdf
[4]https://cryosphericsciences.org/publications/snow-classification/

south-side of the plateau. Weather conditions were optimal during all the tests.

On the surface, at the snow-air interface, there is a 3 cm layer (H=47-44 cm above ground) of poorly cohesive wet snow characterized by rounded cluster grains (F=6a; E=1.0 mm; R=1), generated by positive air temperatures (T_a +9°C) resulting in surface snow warming (T_N at H=45 cm 0.0°C). Continuing down the snow profile, there is a hard melt-freeze crust (H=44-42 cm; F=6; E=0.8 mm; R=5). Below this initial crust, there are 12 cm of faceted crystals and rounded faceted grains (H=42-30 cm; F=4c-4a; E=1.0-1.2 mm; R=2). These are crystals that have undergone constructive metamorphism with kinetic growth, with a predominance of crystals with facets and edges undergoing rounding (F=4c) compared to rounded faceted grains (F=4a). Subsequently, another layer of faceted grains was observed (H=30-20 cm; F=4a-4c; E=1.5-1.0 mm; R=1), similar to the previous layer but with a predominance of rounded faceted grains (F=4a) compared to grains with facets and edges undergoing rounding (F=4c). Beneath these layers, there exists a 2 cm melt-freeze crust (H=20-18 cm; F=6; R=5) formed before the last snowfall. Below this crust, 8 cm long kinetically grown crystals consisting of depth hoars (F=5a) and rounded faceted grains (F=4a) were detected (H=18-10 cm; F=5a, 4a; E=3.0-1.0 mm; R=1). Finally, the basal layer at the snow/ground interface consists of a thick and resilient crust (H=10-0 cm; F=6; R=5).

IV. Experimental Results and Discussion

We now discuss the obtained results from the experimental tests. We conducted the two following types of tests.

- Reference locations (RL).
- Maximum distance propagation (MDP).

A. Results

Concerning the RL test, we deployed one transmitter buried under 42 cm of snow on the plateau and four receivers, two of which were used as back-up units. The reference locations were marked with wooden stakes, and the layout of the RL test is shown in Fig. 3. Each reference location is positioned 10 m from the previous location. Receiver 1 is positioned on the south-side of the plateau, while Receiver 2 is on the north-side of the plateau.

For each reference location, we gather data from both receivers during a 1-minute data collection period and we analyze the RSS and SNR variations. Concerning the RSS, we show in Fig. 4 how the RSS varies. As expected, the RSS decreases with increasing distance from the transmitter. For Receiver 1, we observe a variation from -79 dBm at a 10 m distance to -98 dBm at a 50 m distance. A distinct pattern emerges as we transition from distances of 10 m to 20, 30, 40, and 50 m. Specifically, the median RSS decreases from -70 dBm at 10 m to -90 dBm at 20 m, maintaining a consistent range within this interval up to 50 m. More specifically, there is an approximate 11 dBm decrease in RSS

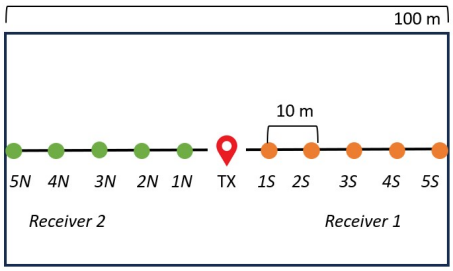

Fig. 3: Experimental layout. The red pin shows the transmitter's position, while the orange dots indicate Receiver 1's reference locations (south-side) and the green dots indicate Receiver 2's reference locations (north-side).

TABLE IV: Statistics of the RSS for Receiver 1 and 2 and for each reference location.

Distance	Receiver 1		Receiver 2	
	Median [dBm]	90th [dBm]	Median [dBm]	90th [dBm]
10 m	−79	−79	−82	−81
20 m	−90	−89	−86	−85
30 m	−92	−92	−88	−88
40 m	−95	−94	−91	−91
50 m	−98	−97	−95	−95

values from 10 m to 20 m, followed by an 8 dBm decrease from 20 m to 50 m. Concerning Receiver 2 such pattern is not so evident, with a decrease of 4 dBm from 10 m to 20 m and a decrease of 9 dBm from 20 m to 50 m. One potential explanation for this variance could be the varying alignment of the transmitter's antenna in relation to Receivers 1 and 2.

Given a specific distance, we also observe that the RSS tends to remain stable. This observation is confirmed by the data reported in Table IV. The table shows the median and 90*th* percentile of the RSS for each reference location and for each receiver.

Concerning the quality of the LoRa channel, Fig. 5 shows the SNR variation for each reference location and for each receiver. The figure shows that the channel is not significantly disturbed when the SNR is always greater than 9 dB, as also reported in Table V.

Concerning the MDP test, the goal was to measure the maximum distance at which we are able to collect LoRa messages broadcasted by the transmitter. For this purpose, we walked toward the south with respect to the transmitter's location, and we marked 10 waypoints to keep track of the followed path, as shown in Fig. 6. Waypoints are labelled in the range of 1-10 in Fig. 6, and the transmitter location is labelled as *TX*. The path is not straight due to obstacles along the way, such as trees or slopes. The receiver stopped recording any LoRa signal at 414 m from the transmitter location. In the figure, we also show how the RSS degrades as the receiver moves away from the transmitter location. The RSS varies between -70 dBm at 0 m from the transmitter (TX label) and -136 dBm at 414 m from the transmitter (labels 9 and 10 in Fig. 6b). We observe an initial decrease

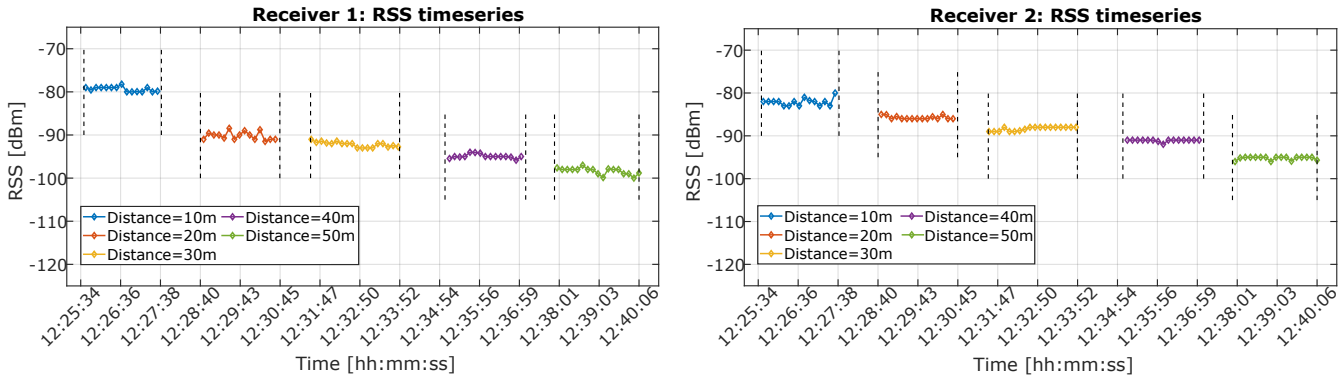

Fig. 4: RSS variation for Receiver 1 and 2 at the reference locations.

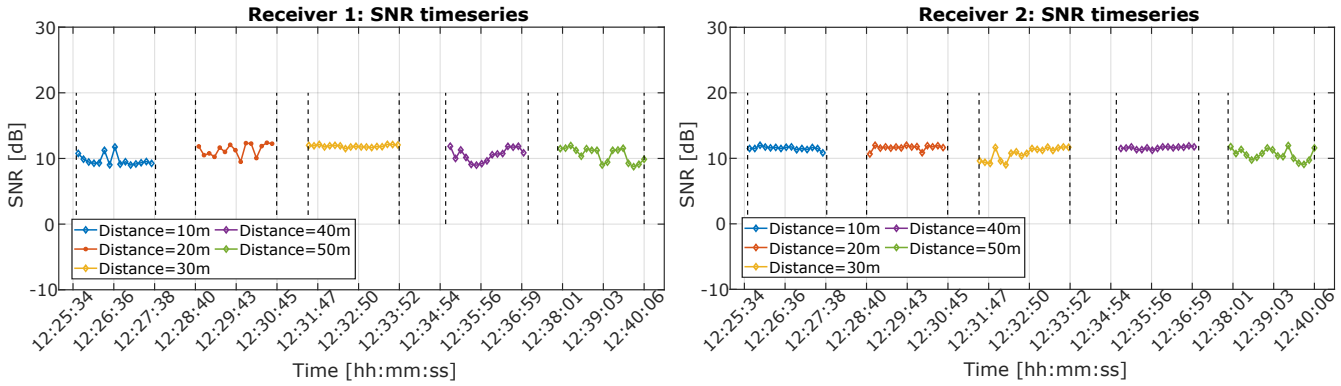

Fig. 5: SNR variation for Receiver 1 and 2 at the reference locations.

TABLE V: STATISTICS OF THE SNR FOR RECEIVER 1 AND 2 AND FOR EACH REFERENCE LOCATION.

Distance	Receiver 1		Receiver 2	
	Median [dB]	90th [dB]	Median [dB]	90th [dB]
10 m	9.5	11.1	11.5	11.75
20 m	11.5	12.25	11.75	12
30 m	11.75	12	11.25	11.75
40 m	10.25	12	11.625	11.75
50 m	11.25	11.5	10.25	11.75

in the RSS value when moving from the label TX to label 1, after which the RSS smoothly decreases up to the maximum distance. The SNR also reflects the signal attenuation due to the distance of the obstacles, ranging from 12 dB (clear channel) in the TX to -9.7 dB in label 10 (disturbed channel).

B. Discussion

From the executed tests we derive some considerations that motivate us to further investigate the use of LoRa in SAR operations.

RSS and SNR stability. We observe that the RSS and SNR values remain stable when collecting data from the reference locations. This capability enables the creation of a resilient system capable of mitigating unexpected fluctuations even under stable conditions, thereby facilitating SAR

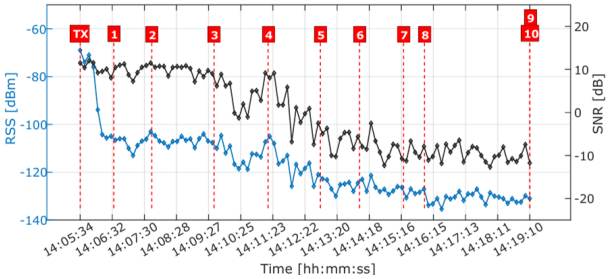

(a) Variation in the RSS and SNR during the MDP test. The red labels correspond to the waypoints collected during the test.

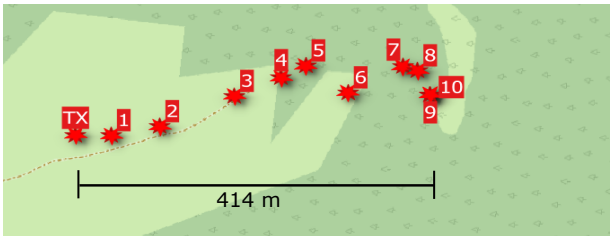

(b) Path followed during the MDP test.

Fig. 6: Layout of the MDP test.

operations in critical scenarios. However, we observed a discernible RSS threshold when transitioning from a distance of 10 m to greater distances, such as 20 m or more. This indicates the necessity of gathering data at locations closer to the transmitter. Consequently, we intend to expand our data collection campaign by incorporating a greater number of reference points, including close-range locations (from 30 cm to 3 m) and distant locations (from 10 m to 50 m).

Lack of direction estimation. The adopted LoRa hardware only includes omnidirectional antennas, which do not allow estimation of the signal direction of LoRa messages from the transmitter. For the successful use of LoRa in avalanche scenarios, we consider a promising approach to test directional antennas, such as the Yagi antenna still modulating at 868 MHz or the use of technologies estimating the Angle of Arrival [21].

Multiple technologies in avalanche scenarios. The insights we gleaned during data collection prompted us to view LoRa as a complementary technology alongside ARVA systems. The standout ability of LoRa lies in its ability to cover extensive distances, as demonstrated by the Maximum Distance Propagation test. Conversely, ARVA excels in precision distance estimation within close ranges, ranging from 5 m to 30 cm from the transmitter's location. Consequently, we envision a promising strategy involving the integration of the strengths of both technologies to develop a next-generation rescue device equipped with multiple receivers.

V. Conclusions

This work presents a novel experimental approach to thoroughly characterize LoRa propagation in the challenging scenario of avalanche search and rescue (SaR), where the transmitter is buried under snow. We address key aspects of this scenario, including the snow complete characterization, the absence of a line-of-sight between transmitter and receiver and signal attenuation due to environmental factors such as temperature, humidity, and snow conditions. Through our data collection campaign involving one transmitter and four receivers, we conducted comprehensive tests to assess LoRa propagation. Our findings shed light on the performance of LoRa technology in SaR scenarios, demonstrating its potential in overcoming communication challenges in harsh environments. By analyzing the variations in the Received Signal Strength (RSS) and Signal-to-Noise Ratio (SNR) with increasing distance between the transmitter and receiver and testing the maximum reception distance from a buried transmitter, we provide valuable insights into the capabilities of LoRa technology under such demanding conditions.

Acknowledgments

The authors thank ARPAV (Unità Organizzativa Neve, Valanghe e Stabilità dei Versanti - Centro Valanghe di Arabba) for their support for the snow profile characterization. This work is partially funded by STRIVE Project CUP: B53C22010110001 by MUR ministry. The research described in this article was conducted under an agreement between DICII-Tor Vergata, and ISTI-CNR researching "Remote Radio Frequency Identification systems for Health and Safety applications through radiolocation and machine learning techniques".

References

[1] L. Slats, https://blog.semtech.com/a-brief-history-of-lora-three-inventors-share-their-personal-story-at-the-things-conference, 2020.

[2] Z. Sun, H. Yang, K. Liu, Z. Yin, Z. Li, and W. Xu, "Recent advances in LoRa: A comprehensive survey," *ACM Trans. Sensor Netw.*, vol. 18, no. 4, 2022.

[3] G. Pasolini, "On the LoRa Chirp Spread Spectrum modulation: Signal properties and their impact on transmitter and receiver architectures," *IEEE Tran. Wire. Commun.*, vol. 21, no. 1, p. 357 – 369, 2022.

[4] M. Alipio and M. Bures, "Current testing and performance evaluation methodologies of LoRa and LoRaWAN in IoT applications: Classification, issues, and future directives," *Internet of Things*, vol. 25, 2024.

[5] J.-M. Kang, "On the LoRa modulation for IoT: Preamble designs for channel estimation with single-and multi-chirp transmission strategies," *IEEE Internet of Things J.*, p. 1–13, 2024.

[6] G. M. Bianco, R. Giuliano, G. Marrocco, F. Mazzenga, and A. Mejia-Aguilar, "LoRa system for search and rescue: Path-loss models and procedures in mountain scenarios," *IEEE Internet of Things J.*, vol. 8, no. 3, pp. 1985–1999, 2021.

[7] I. Cappelli, G. Di Renzone, A. Fort, M. Mugnaini, A. Pozzebon, and V. Vignoli, "Long range (LoRa) transmission through ice: Preliminary results," in *Conf. Record - IEEE Instrum. Meas. Technol. Conf.*, 2021.

[8] G. M. Bianco and G. Marrocco, "Body-UAV near-ground LoRa links through a mediterranean forest," *IEEE Tran. Antennas Propag.*, vol. 71, no. 7, p. 6214 – 6218, 2023.

[9] F. Potorti *et al.*, "Localising crowds through Wi-Fi probes," *Ad Hoc Networks*, vol. 75-76, pp. 87–97, 2018.

[10] M. Girolami, F. Mavilia, A. Berton, G. Marrocco, and G. Maria Bianco, "An experimental dataset for search and rescue operations in avalanche scenarios based on lora technology," *IEEE Access*, vol. 12, pp. 171 015–171 035, 2024.

[11] M. N. Soorki, H. Aghajari, S. Ahmadinabi, H. B. Babadegani, C. Chaccour, and W. Saad, "Catch me if you can: Deep meta-RL for search-and-rescue using LoRa UAV networks," *Lecture Notes Netw. Sys.*, vol. 674 LNNS, p. 115 – 119, 2023.

[12] A. Calabro and E. Marchetti, "Improving SAR ops using Wi-Fi and LoRa on UAV," in *IEEE Int. Conf. Perv. Comp. Commun. Work. Aff. Events, PerCom Work.*, 2022, p. 82 – 84.

[13] M. Thomeczek, "Live GNSS tracking of search and rescue dogs with LoRa," *Lecture Notes Netw. Sys.*, vol. 674 LNNS, p. 115 – 119, 2023.

[14] M. Z. S. Hadi, A. A. Dafa, and P. Kristalina, "Detection of dead victims at volcanic disaster location based on drone and LoRa," in *Proc. Int. Conf. Comp. Eng., Netw. Int. Multimedia*, 2022, p. 213 – 217.

[15] G. M. Bianco, R. Giuliano, F. Mazzenga, and G. Marrocco, "Multi-slope path loss and position estimation with grid search and experimental results," *IEEE Tran. Signal Inf. Proc. Netw.*, vol. 7, pp. 551–561, 2021.

[16] C. Bouras, A. Gkamas, and S. Aniceto Katsampiris Salgado, "Exploring the energy efficiency for search and rescue operations over LoRa," in *11th IFIP Int. Conf. New Technol., Mob. Secur.*, 2021.

[17] M. P. Manuel, M. Faied, and M. Krishnan, "A novel LoRa LPWAN-based communication architecture for Search & Rescue missions," *IEEE Access*, vol. 10, p. 57596 – 57607, 2022.

[18] R. Niu, A. Vempaty, and P. K. Varshney, "Received-signal-strength-based localization in wireless sensor networks," *Proc. IEEE*, vol. 106, no. 7, p. 1166 – 1182, 2018.

[19] LILYGO, https://www.lilygo.cc/products/t-beam-v1-1-esp32-lora-module, 2024.

[20] LILYGO, https://www.lilygo.cc/products/gsm-gprs-antenna, 2024.

[21] M. Girolami, F. Furfari, P. Barsocchi, and F. Mavilia, "A Bluetooth 5.1 dataset based on angle of arrival and RSS for indoor localization," *IEEE Access*, vol. 11, pp. 81 763–81 776, 2023.